

RSC Advances



This is an *Accepted Manuscript*, which has been through the Royal Society of Chemistry peer review process and has been accepted for publication.

Accepted Manuscripts are published online shortly after acceptance, before technical editing, formatting and proof reading. Using this free service, authors can make their results available to the community, in citable form, before we publish the edited article. This *Accepted Manuscript* will be replaced by the edited, formatted and paginated article as soon as this is available.

You can find more information about *Accepted Manuscripts* in the [Information for Authors](#).

Please note that technical editing may introduce minor changes to the text and/or graphics, which may alter content. The journal's standard [Terms & Conditions](#) and the [Ethical guidelines](#) still apply. In no event shall the Royal Society of Chemistry be held responsible for any errors or omissions in this *Accepted Manuscript* or any consequences arising from the use of any information it contains.

Highly Heat-Resistant and Thermo-Oxidative Stability of Borosilane Alkynyl Hybrid Polymers

Hua Zhou, Quan Zhou^{*}, Qi Zhou, Lizhong Ni and Qi Chen^{*}

** Correspondence to: Quan Zhou and Qi Chen, E-mail: qzhou@ecust.edu.cn; chenqi@ecust.edu.cn.*

School of Materials Science and Engineering, Key Laboratory of Special Functional Polymeric Materials and Related Technology of the Ministry of Education, East China University of Science and Technology, Shanghai 200237, People's Republic of China.

Abstract: A kind of boron-silicon-containing hybrid polymers with C≡C units (HBS) were prepared, and the effects on the properties of the polymers with three different substituents were studied. The polymers were synthesized with ethynylmagnesium bromide, dichlorosilane and boron fluoride etherate by using Grignard reagent method. The structures of HBS were characterized by fourier transform infrared spectra (FTIR), ¹H-NMR, ¹³C-NMR, ²⁹Si-NMR, and gel permeation chromatography (GPC). Thermal and oxidative stabilities were studied by differential scanning calorimetry (DSC) and thermal gravity analysis (TGA), and the cross-linking reaction mechanisms of the HBS were discussed. All the polymers exhibit excellent thermal and oxidation resistance, particularly, HBS-1 with Si-H bonds showed highly heat-resistant and thermo-oxidative stability; the temperature of 5% weight loss (T_{d5}) were 624°C and 607°C in nitrogen and air respectively, and the residues at 1000°C were 86.8% and 77.5% respectively. The thermal and oxidative stabilities of the polymers were attributed to the synergistic effect of boron and silicon elements and the cross-linking reactions of hydrosilylation and Diels-Alder reactions.

Key Words: Borosilane alkynyl hybrid; thermal oxidation resistance; curing behavior.

INTRODUCTION

Inorganic-organic hybrid polymers, especially silicon-containing polymers, have been studied for several years, because of its unique properties that as hard, highly heat-resistant as ceramics and as moldable, soluble as plastics ^[1-2]. The silicon-based polymers have many applications in different fields, such as ceramic precursor, coating materials, electronic materials, matrix composites and components in space vehicles ^[3-6]. Itoh et al. ^[7-10] has been focused on the research of silicon-containing polymers for years. They synthesized poly(phenylsilyleneethynylene-1,3-phenyleneethynylene)(MSP), which was prepared by the dehydrogenative coupling polymerization reaction between phenylsilane and m-diethynylbenzene. The results showed that the T_{d5} of the polymer was greater than 800°C, and the residue at 1000°C were 90% and 25.5% under inert and air atmospheres, respectively. Homrighausen et al.^[11] synthesized a linear silarylene-siloxane-diacetylene polymer which was prepared via polycondensation of 1,4-bis(dimethylaminodimethylsilyl)butadiyne with 1,4-bis(hydroxydimethylsilyl)benzene, and the results showed that the polymer exhibited long-term thermo-oxidative stability up to 350°C in air. Although the silicon-containing polymers have highly heat-resistance property, the thermal oxidation performance needs to be improved.

In recent years, the incorporation of inorganic elements such as boron into organic polymer also has been researched. Yajima et al.^[12] synthesized poly(boro-diphenylsiloxane) through the reaction of boric acid and diphenyldichlorosilane or diphenylsilanediol and observed the process of its thermal decomposition. Sundar et al.^[13] synthesized a linear

boron-silicon-diacetylene copolymers that had weight residues above 50% at 1000°C in air, and the hybrid systems showed outstanding thermal oxidative properties compared to commercial organic systems. Deepa et al.^[14] synthesized a kind of boronsiloxane oligomers through the condensation of boric acid with phenyltrimethoxysilane and phenyltriethoxysilane, and the results showed that the oligomers gave ceramic residues in the range of 64-75% (at 900°C in inert atmosphere).

In our preliminary study, we reported some novel linear silicon-containing hybrid polymers with $C\equiv C$ units which showed excellent thermal and oxidative stabilities^[15-19]. And synthesized phenyl acetylene terminated poly (carborane-silane) (PACS) by the couple reaction of methylchlorosilane with 1,7-dilithio-m-carborane and lithium phenylacetylide, which exhibits extremely thermal and oxidative property^[20]. Nevertheless, the relative high cost of carborane limited the utilization and development of polymers.

Based on these factors, further performance on thermal oxidation enhancement of silicon-containing polymers is strongly expected. An effective approach for the performance enhancement is introducing another inorganic element, and the hybrid of boron has become increasingly attractive. In this paper, three kinds of borosilane alkynyl hybrid polymers with different substituent groups were synthesized. The characterization of the three polymers, thermoset mechanism and thermal oxidation properties were discussed.

EXPERIMENTAL

Materials

All reactions were performed under inert conditions of dry nitrogen because the starting materials were sensitive to oxygen and moisture. THF was distilled from

benzophenone/sodium before use. Ethynylmagnesium bromide (0.5 mol L^{-1} in THF) was purchased from Sinopharm Chemical Reagent Co.(Shanghai, China) and titrated before use. Dichloromethylsilane, dimethyldichlorosilane, diphenyldichlorosilane and boron fluoride etherate were obtained from Aldrich Chemical Co.(Shanghai, China). All other chemicals were reagent grade and used as required.

Synthesis of HBS

A flame-dried 500 mL round-three-necked flask, connected to an argon source, was equipped with a stirrer. Magnesium metal ribbon (1.8 g, 0.075 mol), a small piece of iodine and THF (20mL) were added into the flask. A solution of ethyl bromide (7.63 g, 0.07 mol) in THF (50 mL) was introduced via dropping funnel over a 30 min period, with stirring. After completing addition, the reaction mixture was refluxed for 2 h to produce ethylmagnesium bromide. Then ethynylmagnesium bromide (130 mL, 0.065mol) was added into the reaction system over 30 min, and the reaction was refluxed for 2 h to afford a white mixed organic magnesium reagents (**1**).

Polymer HBS-1 A solution of dichloromethylsilane (0.03 mol) in THF (10 mL) was dropwise introduced to the reaction system (**1**) over 30 min with stirring. White precipitates of the organic magnesium reagent immediately disappeared before the completion of the addition, and the solution became almost clear. The reaction mixture was refluxed for 3 h to get silicon-based acetylene polymers (**2**). Then boron fluoride etherate (0.02 mol) in THF (10 mL) was added. After addition, the reaction mixture was further reacted for 5 h. After that, hydrochloric acid aqueous solution was slowly added through the dropping funnel (over 30 min). The resulting oil phase was extracted with ethyl acetate, then separated using a

separatory funnel and washed with deionized water until to neutral. Then dry the oil phase by adding sodium sulfate. After evaporation of the solvent, a yellowish viscous product with yields of 73% was obtained.

Polymer HBS-2 and HBS-3 A solution of dimethyldichlorosilane (0.03 mol) (synthesis of HBS-2) or diphenyldichlorosilane (0.03 mol) (synthesis of HBS-3) in THF (10 mL) was added dropwise to the reaction system (**1**). Other steps were the same as the synthesis of HBS-1, and yellowish-brown viscous products with yields of 75-78% were obtained.

Measurements

Fourier transform infrared (FTIR) spectra were measured on a Nicolet 6700 spectrometer from KBr pellets for solid samples and films deposited on KBr plates for liquid samples. $^1\text{H-NMR}$, $^{13}\text{C-NMR}$ and $^{29}\text{Si-NMR}$ spectra were recorded on a Bruker Avance 500 spectrometer (500 MHz for $^1\text{H-NMR}$, 125.77 MHz for $^{13}\text{C-NMR}$ and 500 MHz for $^{29}\text{Si-NMR}$), with tetramethylsilane as the internal reference. Molecular weights were determined by gel permeation chromatography (Waters 1515), using THF as eluent at a flow rate of 1.0 mL min^{-1} and polystyrene as the standard. The viscosities were recorded on Brookfield CAP 2000+ instrument at 25°C . Differential scanning calorimetry (DSC) measurements were performed on NETZSCH DSC 200 F3 instrument at a heating rate of $10^\circ\text{C min}^{-1}$ under nitrogen atmosphere. Rotational rheometer measurements were performed on Thermo Haake RS600 with shearing rates of 0.01 s^{-1} . Thermo gravimetric analyses (TGA) were performed on a PerkinElmer Pyris Diamond from 30 to 1000°C using heating rates of $10^\circ\text{C min}^{-1}$ under nitrogen atmosphere with flow rates of 20 mL min^{-1} . The morphologies of curing polymers were observed by scanning electron microscope (SEM) equipment, S-3400N.

RESULTS AND DISCUSSION

Synthesis and characterization of HBS

The polymers were generated via polycondensation reactions using Grignard reagent method and the synthetic routes are summarized in Scheme 1. The structures of HBS were confirmed by FTIR, $^1\text{H-NMR}$, $^{13}\text{C-NMR}$ and $^{29}\text{Si-NMR}$ spectra and the relevant data are shown in Table I, which proves that the obtained polymers are consistent with the designed structures.

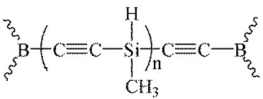
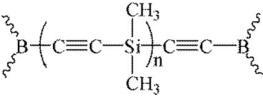
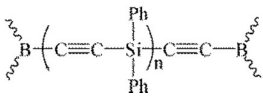
The FTIR spectra of HBS are shown in Fig.4, curve a, c, e exhibits spectrum of HBS-1, HBS-2 and HBS-3 respectively. The characteristic stretching and deformation bands of all expected motifs as illustrated in Table I. By comparing the three cures, a sharper and stronger absorption for HBS-1 than HBS-2 and HBS-3 at 2170 cm^{-1} is observed, which is attributed to the overlap of Si-H group and B-C \equiv C group. Without the Si-H group, HBS-2 and HBS-3 have a weak absorption peak at 2150 cm^{-1} of B-C \equiv C group. In addition, three polymers have a strong absorption peak at 2040 cm^{-1} which is a characteristic peak of Si-C \equiv C group. Besides, all polymers show absorptions around 1410 cm^{-1} (B-C) and 1250 cm^{-1} (Si-C) region which reflect the presence of boron and silicon.

The NMR spectra of HBS-1 are depicted in Fig.1. In the $^1\text{H-NMR}$ spectrum, HBS-1 shows a broad signal centred at 0.45 ppm which is attributed to the Si-CH $_3$ groups. A resonance assigned to Si-H proton is observed at 4.34 ppm. The spectrum of $^{13}\text{C-NMR}$ shows a broad signal at -2.61 ppm assigned to Si-CH $_3$ sites, and the C \equiv C bond is identified in 83.43 ppm region. The introduction of Si element is shown by signals at -62.6 ppm in $^{29}\text{Si-NMR}$ spectrum. The NMR spectra data of HBS-2 and HBS-3 are summarized in Table I.

Pale yellow to brown viscous liquid polymers were obtained from HBS-1 to HBS-3. The

polymers were highly soluble in many general organic solvents such as tetrahydrofuran (THF), toluene, acetone and chloroform. The molar mass (number-average molar mass M_n), molecular weight distribution (M_w / M_n) and viscosity of HBS are shown in Table I. The molecular weight of HBS-1 is the highest among the three polymers, which is attributed to the small units of Si-H in the backbone that is easier to rotate and move to form long molecular chain, and then results in increasing of molar mass. Meanwhile, Si-Ph units are rigid groups and have a large space steric hindrance, and the flexibility of Si-CH₃ units is between those of Si-H units and Si-Ph units^[21], leading to the change in viscosity and molar masses of HBS.

Table I. Structure, Spectral Data and Basic Properties of HBS

Sample	Mn(g mol ⁻¹) and distribution	Viscosity (mPa s ⁻¹)	Spectral data			
			FTIR (cm ⁻¹)	¹ H-NMR (ppm)	¹³ C-NMR (ppm)	²⁹ Si-NMR (ppm)
 HBS-1	1786	2560	2955 (-CH ₃)	4.34 (Si-H)	83.43 (C≡C)	-62.6
	1.55		2170 (Si-H, B-C≡C)			
 HBS-2	1509	2880	2954, 2861 (-CH ₃)	0.36-0.53	85.82 (C≡C)	-41.8
	1.25		2155 (B-C≡C)			
 HBS-3	997	3435	2956-3069 (Ph-H)	7.32-7.76	123-136 (Ph)	-52.3
	1.12		2154 (B-C≡C)			
			2040 (Si-C≡C)			
			1482-1663 (Ph)			
			1429 (B-C)			
			1262 (Si-C)			

Curing behavior of HBS

The curing behaviors of the three polymers were examined by DSC and rheometer. From the DSC exothermic curves in Fig. 2, all the polymers (HBS-1, HBS-2, HBS-3) show strong exotherm during 250 ~ 320°C which is a characteristic of the acetylene cross-linking reaction^[6]. It means that these exothermic transformations are related to a chemical process, i.e., a thermally induced cross-polymerization through the acetylene groups which will modify irreversibly the backbone of the polymers. In investigating the thermal polymerization in HBS-1, it was of utmost interest to discuss the thermosetting mechanism.

In these three polymers, the one exception is polymer HBS-1, which displays two exothermic maxima at 150 and 280°C. Due to the high reactivity of the Si-H bonds, the cross-linking is likely to occur at lower temperature. The first exotherm at ca. 150°C could be caused by intermolecular cross-linking reactions between the Si-H and C≡C bonds. As a result, it has cross-linked to form network structures, which leads to stereo hindrance in the thermoset. So the second exotherm caused by acetylene polymerization is at a higher temperature ca. 280°C. HBS-2 and HBS-3 without Si-H bonds have only one exothermic peak respectively, which are caused by Diels-Alder reaction between C≡C bonds. In addition, the different substituent groups in backbone also affect the thermoset of polymers. The steric hindrance of Si-CH₃ groups is smaller compared to the phenyl-substituted polymer, so the exothermic peak shifts to higher temperature with an increase of Si-Ph units in the structure, and the polymer possessing methyl substituents on silicon visually appear to cross-linking at a lower temperature. Finally the exothermic peak above 200°C leads to an order of HBS-3 > HBS-1 > HBS-2, as shown in Fig. 2.

The rheological behavior upon heating was monitored by acquiring the viscosity at different temperatures, and the rheological curves of HBS are shown in Fig. 3. The three curves in the figure all have their respective inflection point, i.e., gel point. When the temperature reaches the gel point, the cross-linking reaction between the acetylene groups get relatively intense and network structure is gradually formed, which leads to the viscosity of the polymer system rises straight up. It can be revealed that the three polymers HBS-1, HBS-2, HBS-3 each has a gel point at 210°C, 255°C and 290°C respectively which is between the initial temperature and peak temperature corresponding to the DSC curves.

To make clear of the curing behavior, FT-IR spectra of polymers cured at 350°C are measured. Fig. 4 shows the vibration absorption change before and after curing of the three polymers. By comparison of curve a and b, c and d, e and f, separately, it suggests that the characteristic vibration bands of Si-H (2170 cm^{-1}) and $\text{C}\equiv\text{C}$ (2040 cm^{-1} , 2170 cm^{-1}) are completely vanished after curing, indicating the completion of the hydrosilylation and Diels-Alder reactions. Curve b for HBS-1 has an absorption peak at 1637 cm^{-1} which is a characteristic peak of $\text{C}=\text{C}$ bond, demonstrating that hydrosilylation reaction occurs, accompanied by generation of a double bond. A strong band is present at 1250 cm^{-1} (Si-C) along with a band of medium intensity at 2900 cm^{-1} (aliphatic C-H stretching vibration) indicate that Si- CH_3 for HBS-1 and HBS-2, Si-Ph for HBS-3 are stable after curing.

Besides, TGA FTIR studies were carried out at a heating rate of $10^\circ\text{C min}^{-1}$ in an air atmosphere from 30 to 420°C . The typical stacked FTIR diagrams of HBS-1 are shown in Fig. 5. At a relatively low temperature ($<100^\circ\text{C}$), the absorption peaks change little. When the temperature increases (100- 250°C), the absorption peaks of Si-H and $\text{C}\equiv\text{C}$ bonds gradually

weaken, which indicates that the hydrosilylation reaction occurred. As temperature continues to rise (250-350°C), these absorption peaks drastically weaken, which reflects that the Diels–Alder reaction occurred. And eventually the absorption peaks disappear when the temperature is up to 400°C which exhaustively demonstrates the completion of the hydrosilylation and Diels–Alder reactions upon heating.

Fig. 6 shows SEM images of the three cured polymers HBS-1, HBS-2 and HBS-3. Glassy density states of the polymers were formed after curing. The surfaces of the three polymers were smooth and no obvious holes observed, which means there is few evolutions of gaseous by-products and volatilization of lower molecular. The addition reaction during curing process creates less pore formation and volatile species, which obviates the problems of extremely exothermic and severe shrinkage.

Thermosetting Mechanism of the polymers

From these results, we conclude that the thermoset mechanism of the three polymers have a difference. The intermolecular cross-linking reactions of HBS-1 are due to the hydrosilylation reaction between Si-H and C≡C bonds, and the Diels-Alder reaction between C≡C proceed above 200°C. The cross-linking reactions of HBS-2 and HBS-3 are attributed to the Diels-Alder reaction between C≡C bonds only (scheme 2). The process of undergo thermally induced cross-polymerization reactions could greatly influence their thermal behavior.

Thermal and oxidative Stabilities of HBS

The thermal and oxidative stabilities of HBS were investigated by TGA under a flow of nitrogen and air respectively, as shown in Figs 7 and 8, and relevant data are summarized in Table II. The TGA traces show that all three polymers exhibited excellent thermal and

oxidation resistant both in nitrogen and air. The weight loss of the HBS occurred mainly between 460 and 650°C, and the T_{d5} values were above 480 and 460°C in nitrogen and air respectively. The char yields at 1000°C were above 72% and 69% in nitrogen and air respectively, which is much higher than MSP^[10] (the residue at 1000°C in air was 25.5%) and PMES^[19] (the residue at 1000°C in air was 47%). Notably, the performance of HBS-1 with Si-H bonds is outstanding. The most obvious feature of HBS is that the residual ratios in the air have been greatly improved.

Table II. TGA Data of Cured HBS in Different Atmospheres

Sample	N ₂		Air	
	T_{d5} (°C)	Residue at 1000°C (%)	T_{d5} (°C)	Residue at 1000°C (%)
HBS-1	624	86.8	607	77.5
HBS-2	485	72.3	467	69.2
HBS-3	595	82.6	543	71.8

The exceptional thermal oxidative stabilities of HBS can be attributed to the barrier effect to oxygen exhibited by boron-silicon alkynyl hybrid systems. First, the condensation reactions of Si-H and C≡C bonds provide the structures of polymers to convert into highly three-dimensional network. The performance for HBS-1 is due to the suppression of the molecular mobility of polymer segments by the bulky cross-linked networks which generated by hydrosilylation reaction and Dials-Alder reaction. For polymer HBS-3, the thermal properties owing to the complex network structure by Dials-Alder reaction and the rigid cyclobenzene groups in the networks. Nevertheless, polymer HBS-2 with methyl units in the chain has a large number of free carbons which are the domination to influence the thermal properties and significantly decreases the residue. With an increase of Si-H units in the C≡C bond-containing structures, the thermal and oxidation resistance are stronger (HBS-1 >

HBS-3 > HBS-2). Besides, when the temperature is higher than 1000°C, the Si, B atoms in the polymers can form inorganic compounds such as SiC, B₄C, SiO₂ and B₂O₃ that are thermally stable and antioxidative^[21]. Based on the results of the above discussion, it indicates that the introduction of silicon and boron elements in the structure as well as the incorporation of Si(H)-C≡C units into backbone can greatly improve the heat and oxidation resistant properties of the polymers.

CONCLUSION

A kind of polymers (HBS) with three different substituent groups that contain boron, silicon elements and C≡C units were synthesized by the condensation reactions using Grignard reagent method in this study. The structures, curing mechanisms, thermal and oxidation resistances of the HBS were characterized. The results showed that the three polymers were highly heat-resistant and especially had excellent oxidation stabilities. Remarkably, the performance of HBS-1 with Si-H units was outstanding compare to the other two polymers that substituted by methyl and phenyl, which with T_{d5} values above 600°C and residues at 1000°C above 75% in nitrogen and air respectively. In addition, the detailed curing mechanisms were discussed. It was suggested that Si(H)-C≡C unit would increase the cross-linking density and the cooperate with inorganic elements of silicon and boron could form the most thermally stable structure.

REFERENCES

1. Chen, J.; Xie, Z.; Lam, J. W. Y.; Law, C. C. W.; Tang, B. Z. *Macromolecules* **2003**, *36*, 1108-1115.
2. Ohshita, J.; Yoshimoto, K.; Hashimoto, M.; Hamamoto, D.; Kunai, A.; Harima, Y. *J.*

- Organomet. Chem.* **2003**, *665*, 29-33.
3. Homrighausen, C. L.; Keller, T. M. *J. Polym. Sci. A: Polym. Chem.* **2002**, *40*, 88-94.
 4. Henderson, L. J.; Keller, T. M. *Macromolecules* **1994**, *27*, 1660-1668.
 5. Kolel-Veetil, M. K.; Beckham, H. W.; Keller, T. M. *Chem. Mater.* **2004**, *16*, 3162-3169.
 6. Itoh, M.; Iwata, K.; Ishikawa, J.; Sukawa, H.; Kimura, H.; Okita, K. *J. Polym. Sci. Part A: Polym. Chem.* **2001**, *39*, 2658-2666.
 7. Itoh, M.; Mitsuzuka, M.; Iwata, K.; Inoue, K. *Macromolecules* **1994**, *27*, 7917-7925.
 8. Itoh, M.; Inoue, K.; Iwata, K.; Ishikawa, J.; Takenaka, Y. *Adv. Mater.* **1997**, *9*, 1187-1193.
 9. Narisawa, M.; Hoshino, J.; Okamura, K.; Itoh, M. *J. Mater. Sci.* **2000**, *35*, 1535-1543.
 10. Itoh, M.; Inoue, K.; Iwata, K.; Mitsuzuka, M.; Kakigano, T. *Macromolecules* **1997**, *30*, 694-702.
 11. Homrighausen, C. L.; Keller, T. M. *Polymer* **2002**, *43*, 2619-2625.
 12. Yajima, S.; Hayashi, J.; Okamura K. *Nature* **1977**, *266*, 521-526.
 13. Sundar, R. A.; Keller, T. M. *Macromolecules* **1996**, *29*, 3647-3653.
 14. Deepa, D.; Packirisamy, S.; Sreejith, K. J.; Ravindran, P. V.; George, B. K. *J. Inorg. Organomet. Polym.* **2010**, *20*, 666-672.
 15. Zhou, Q.; Feng, X.; Ni, L. Z.; Chen, J. D. *J. Appl. Polym. Sci.* **2006**, *102*, 2488-2495.
 16. Zhou, Q.; Feng, X.; Zhao, H. Q.; Ni, L. Z.; Chen, J. D. *J. Appl. Funct. Polym.* **2007**, *1*, 97-105.
 17. Jia L.; Zhou, Q.; Ni, L. Z. *Thermosetting Resin* **2008**, *1*, 11-18.
 18. Zhou, Q.; Ni, L. Z. *J. Appl. Polym. Sci.* **2009**, *112*, 3721-3730.
 19. Chen, M. F.; Xiong, P. L.; Zhou, Q.; Ni, L. Z. *Polym. Int.* **2014**, *63*, 1531-1539.

20. Zhou, Q.; Mao, Z.J.; Ni, L.Z.; Chen, J.D. *J. Appl. Polym. Sci.* **2007**, *104*, 2498-2506.
21. Bedford, S. E.; Yu K.; Windle A. H. *J. Chem. Soc.* **1992**, *88*, 1765-1774.
22. Ijadi-maghsoodi, S.; Barton, T. J. *Macromolecules* **1990**, *23*, 4485-4494.

Captions

Scheme 1. The synthesis routes of HBS

Scheme 2. Possible thermosetting mechanisms of HBS (a) HBS-1; (b) HBS-2 and HBS-3

Table I. Structure, Spectral Data and Basic Properties of HBS

Table II. TGA Data of Cured HBS in Different Atmospheres

Figure 1. ^1H -NMR, ^{13}C -NMR and ^{29}Si -NMR spectra of HBS-1

Figure 2. DSC exothermic curves of HBS (curve a. HBS-1; curve b. HBS-2; curve c. HBS-3)

Figure 3. Rheological curves of HBS (curve a. HBS-1; curve b. HBS-2; curve c. HBS-3)

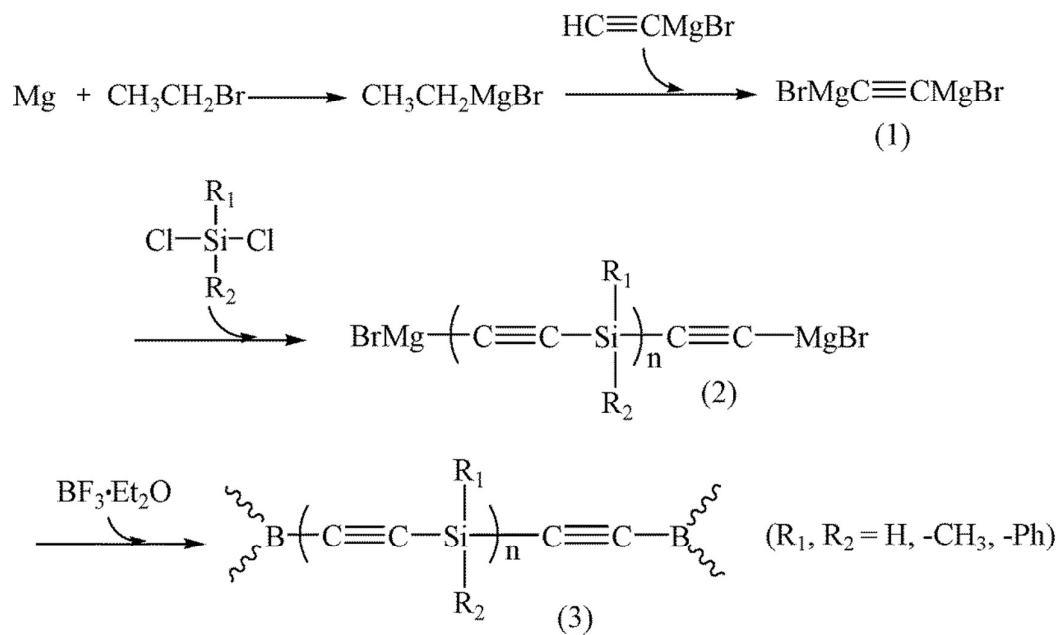
Figure 4. FTIR spectra of HBS (a. HBS-1 before curing, b. HBS-1 after curing; c. HBS-2 before curing, d. HBS-2 after curing; e. HBS-3 before curing, f. HBS-3 after curing)

Figure 5. Stacked FTIR diagrams of HBS-1

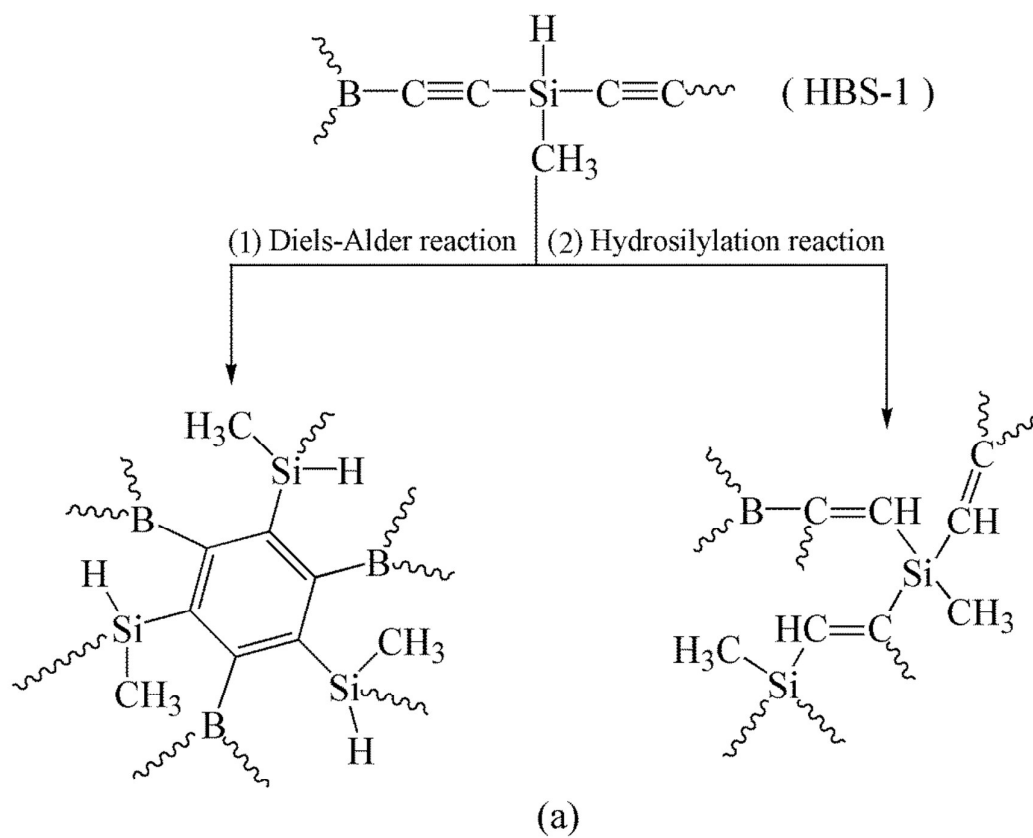
Figure 6. SEM images of (a) HBS-1, (b) HBS-2, (c) HBS-3

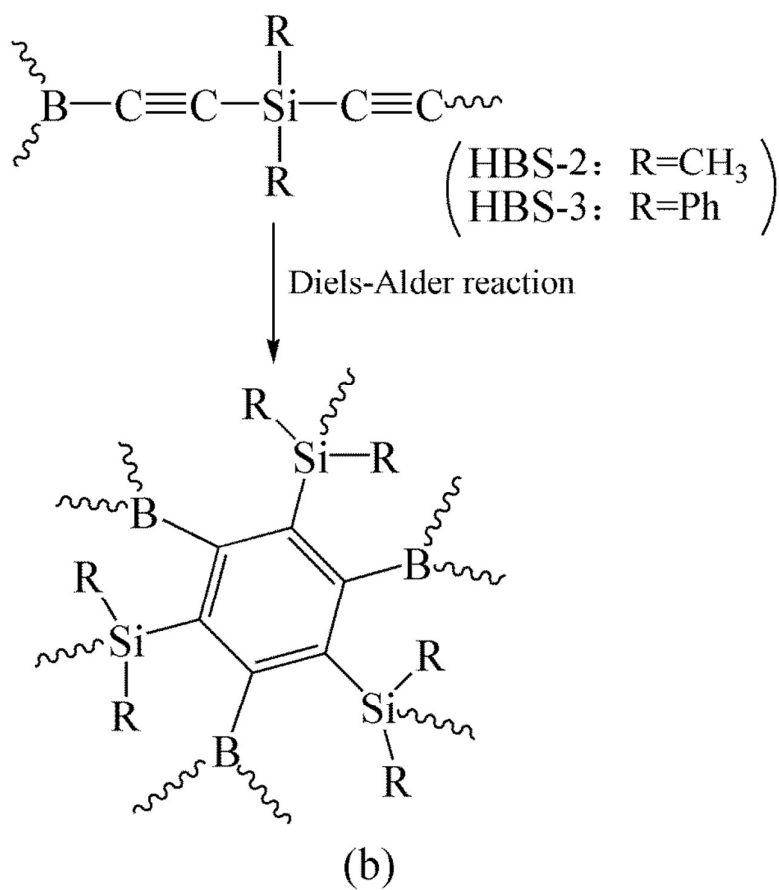
Figure 7. TGA curves of the cured HBS in N_2 (curve a. HBS-1; curve b. HBS-2; curve c. HBS-3)

Figure 8. TGA curves of the cured HBS in air (curve a. HBS-1; curve b. HBS-2; curve c. HBS-3)



Scheme 1. The synthesis routes of HBS





Scheme 2. Possible thermosetting mechanisms of HBS (a) HBS-1; (b) HBS-2 and

HBS-3

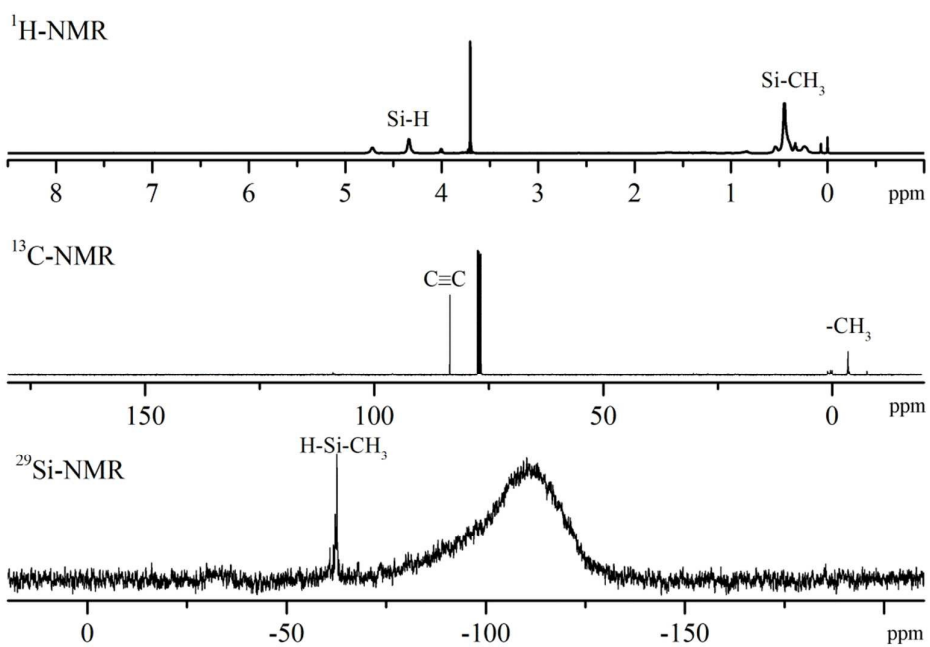


Figure 1. $^1\text{H-NMR}$, $^{13}\text{C-NMR}$ and $^{29}\text{Si-NMR}$ spectra of HBS-1.

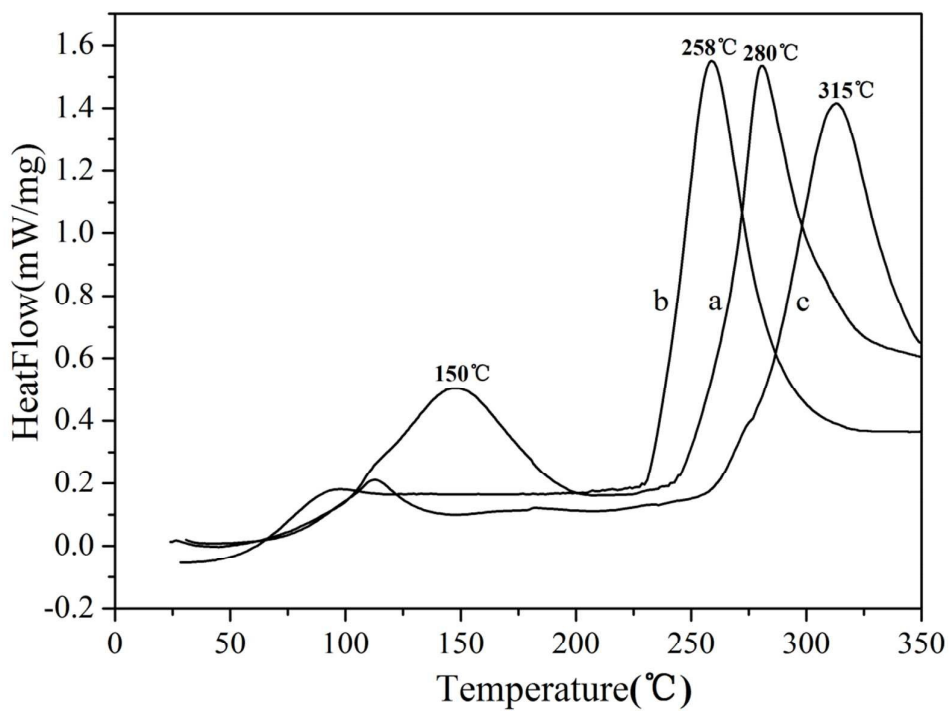


Figure 2. DSC exothermic curves of HBS (curve a. HBS-1; curve b. HBS-2; curve c. HBS-3)

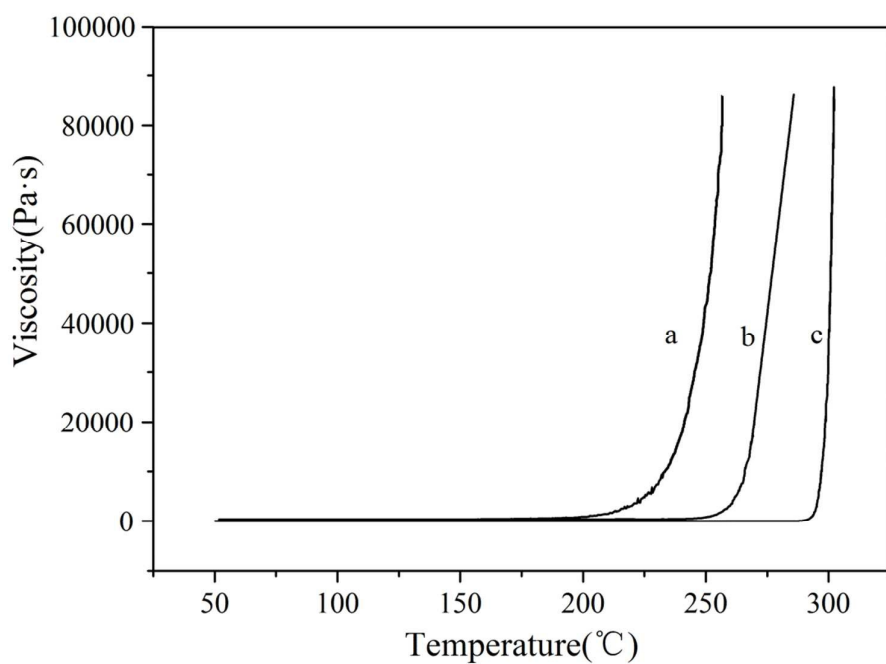


Figure 3. Rheological curves of HBS (curve a. HBS-1; curve b. HBS-2; curve c. HBS-3)

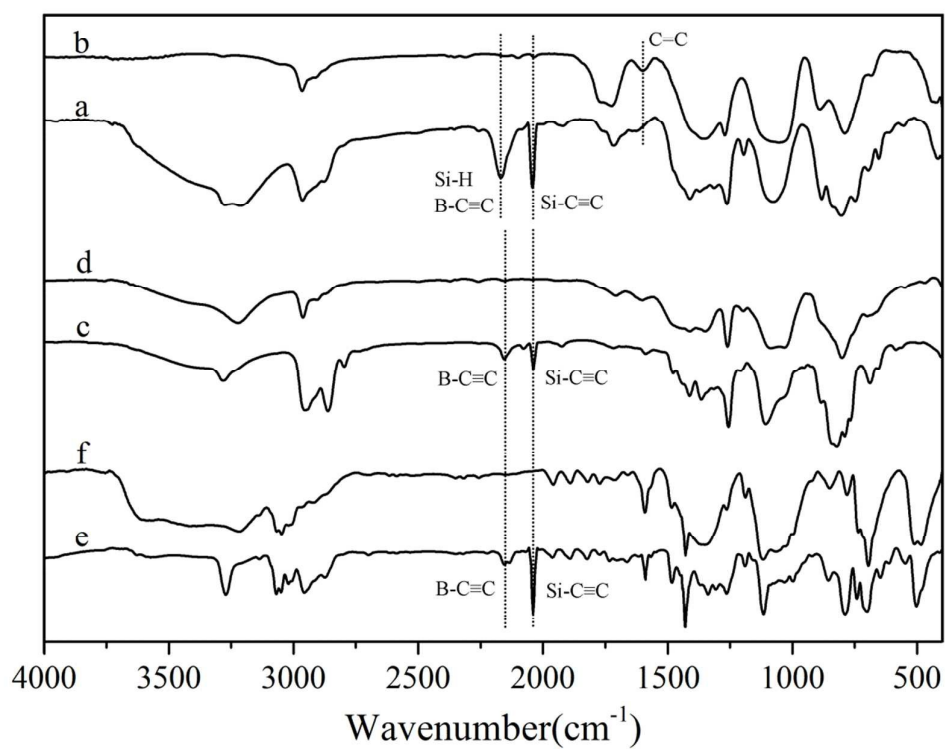


Figure 4. FTIR spectra of HBS (a. HBS-1 before curing, b. HBS-1 after curing; c. HBS-2 before curing, d. HBS-2 after curing; e. HBS-3 before curing, f. HBS-3 after curing)

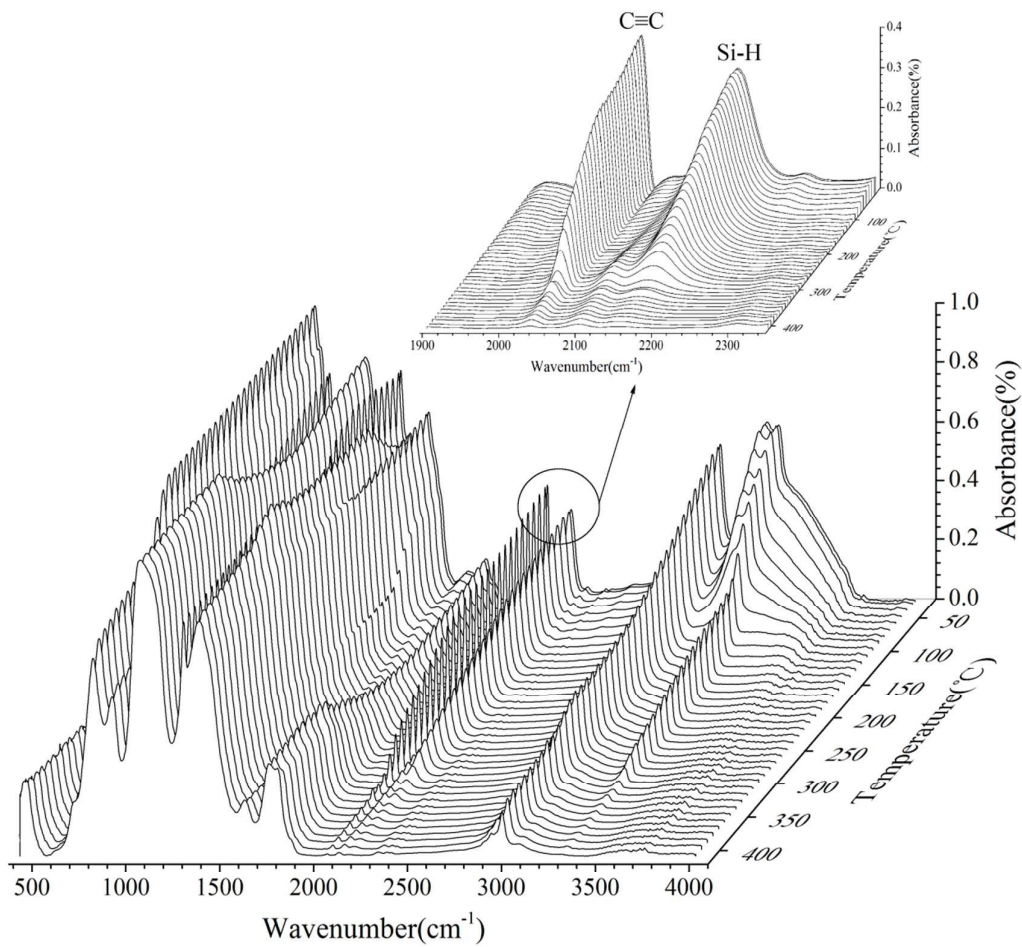


Figure 5. Stacked FTIR diagrams of HBS-1

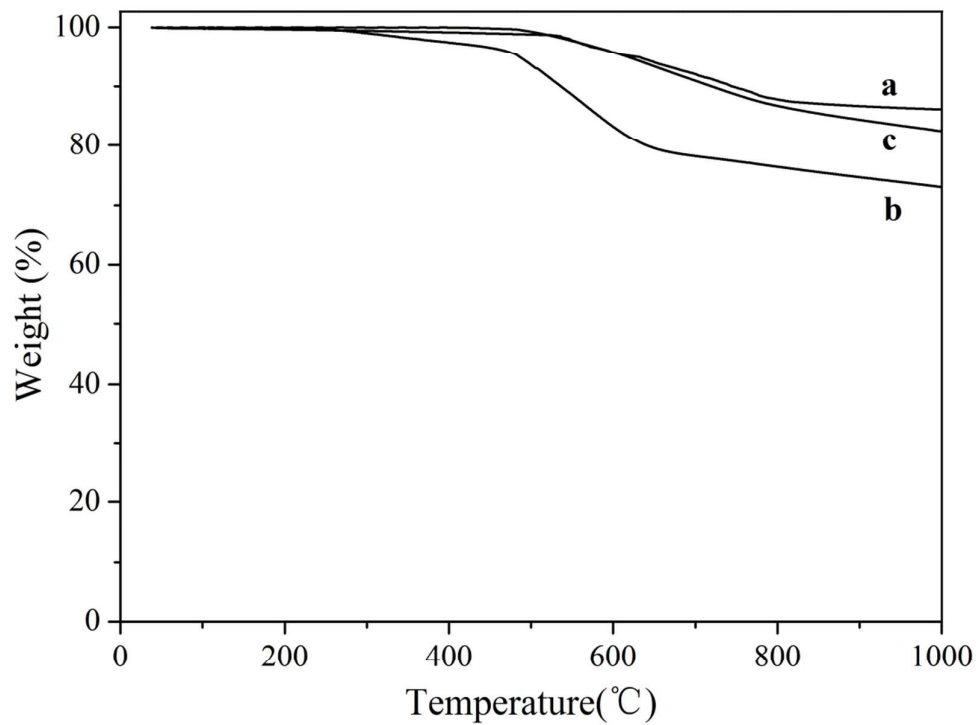


Figure 7. TGA curves of the cured HBS in N_2 (curve a. HBS-1; curve b. HBS-2; curve c. HBS-3)

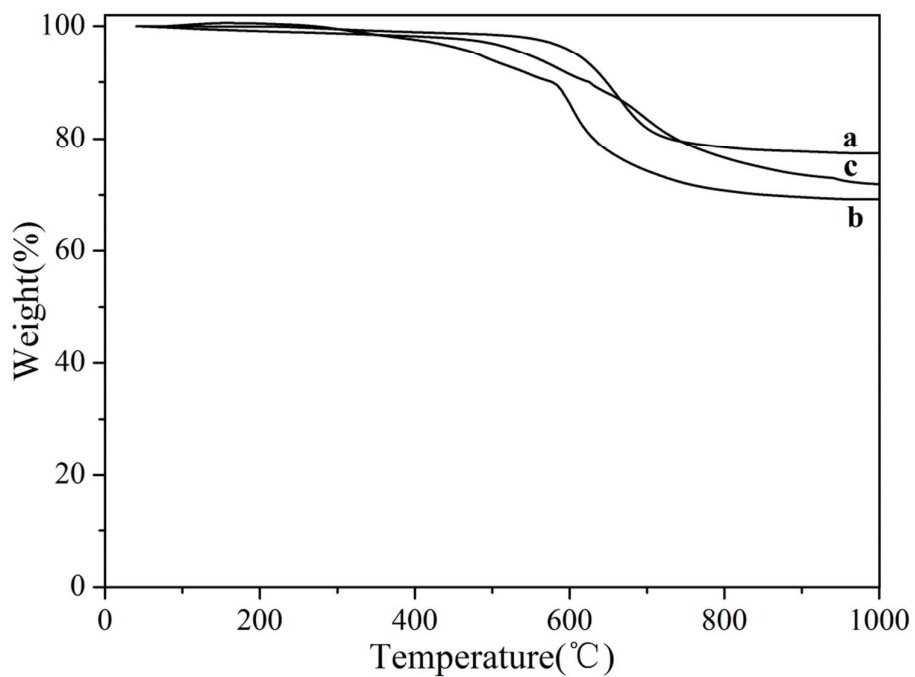
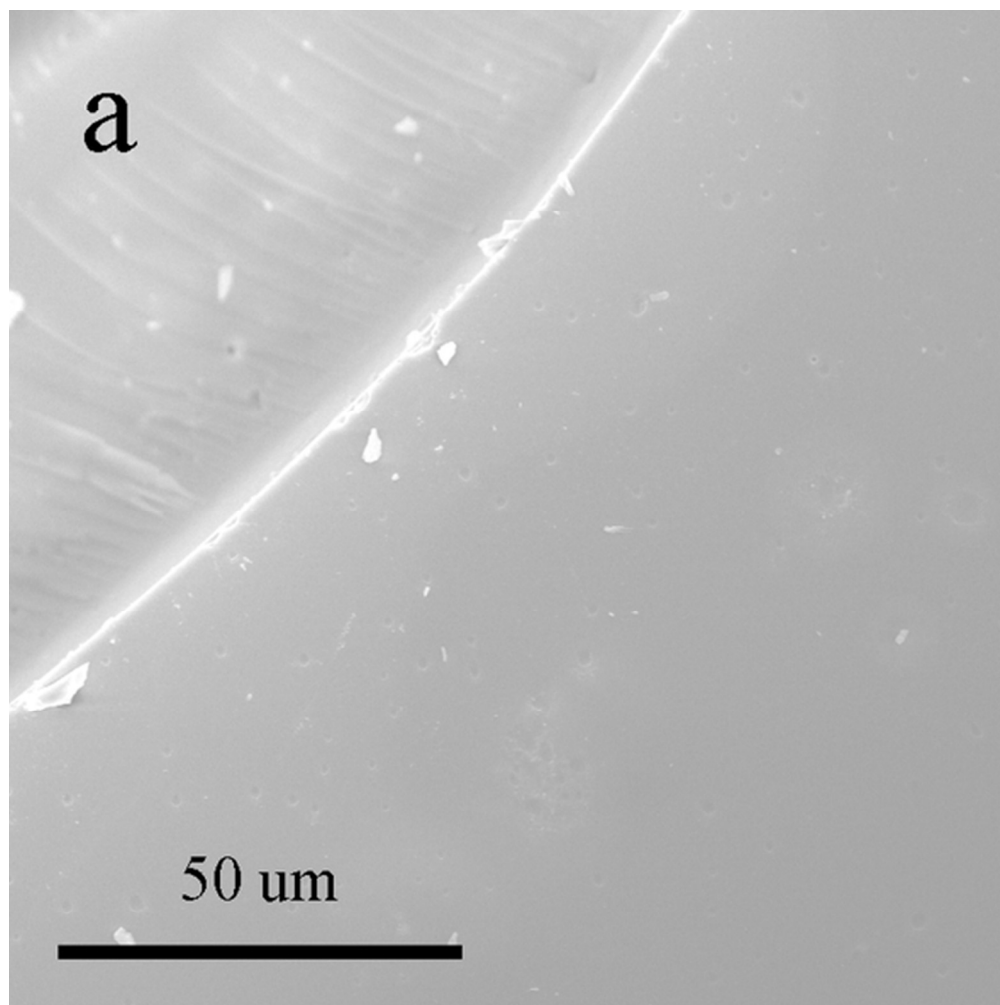
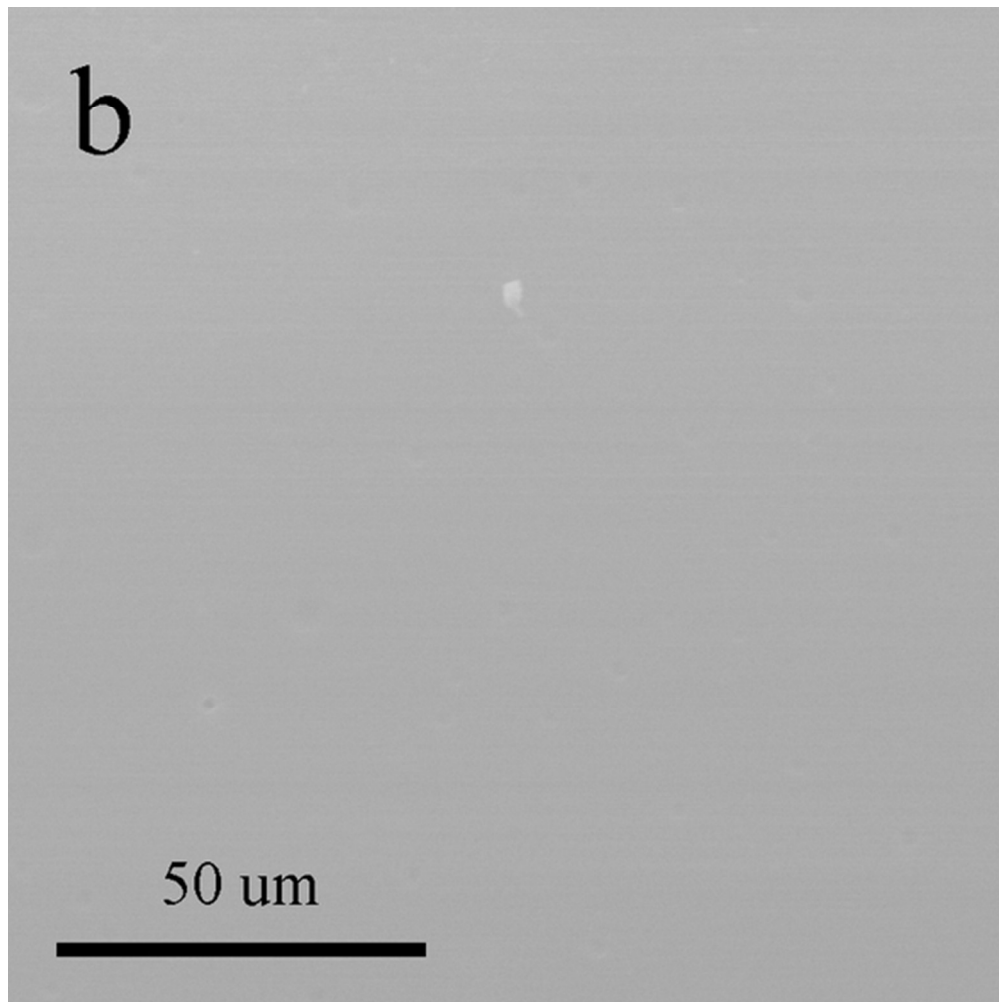


Figure 8. TGA curves of the cured HBS in air (curve a. HBS-1; curve b. HBS-2; curve c. HBS-3)

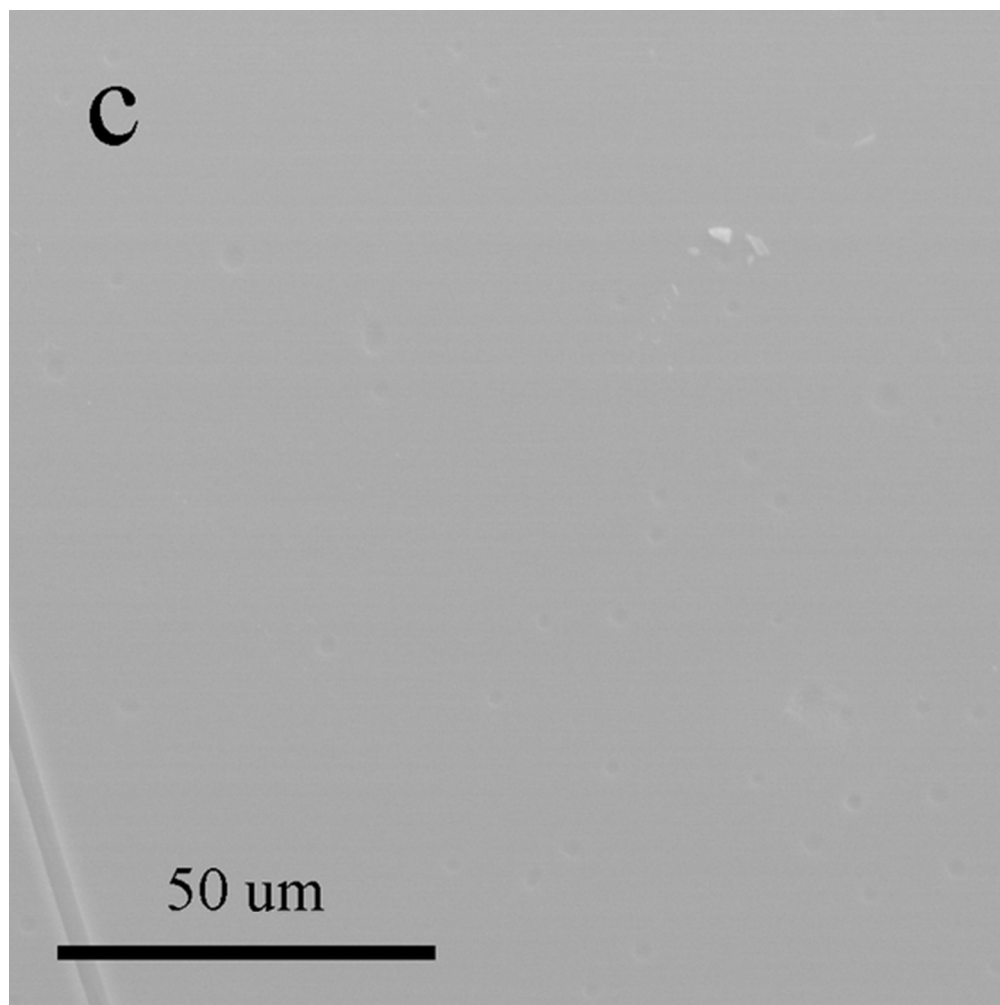


SEM images of (a) HBS-1
50x50mm (300 x 300 DPI)



SEM images of (b) HBS-2

50x50mm (300 x 300 DPI)



SEM images of (c) HBS-3

49x49mm (300 x 300 DPI)